Prediction Capability of Bivariate Statistical Model for the Evaluation of Landslide Probability in Sub-humid and Seismic Active Region of Azad Kashmir, Lesser Himalayas

S.M. Khan[1*], A. Rehman[2], M. Ali[1]

[1]*National Centre of Excellence in Geology, University of Peshawar, Peshawar 25130, Pakistan*

[2]*Department of Geography, University of Peshawar, Peshawar 25130, Pakistan*

A B S T R A C T

Planning and management are necessary tools throughout the world, especially in a mountainous regions where various natural hazards affect the area socially and economically. Landslides are one of the most common natural hazards in mountainous regions throughout the world. For this purpose, qualitative and quantitative methods and landslide susceptibility mapping were used to reduce the probability of landslide occurrence in an affected area and landslide mitigation. The study was focused on landslide susceptibility mapping in Neelum valley using a relative effect model integrated with 17 causative factors of landslides. These factors such as elevation, slope gradient, slope aspect, general curvature, geology, plan curvature, profile curvature, drainage density, stream power index, distance from stream, distance from road, topographic roughness index, Normalized difference wetness index, distance from fault, rainfall, landuse landcover, and Normalized difference vegetative index were used for analysis. Neelum valley is the part of the Himalayan region that is often experiencing landslide hazards frequently. Among other methods, it is a statistical method prepared within the Geographical information system environment to develop landslide hazard zones in Neelum valley. The landslide inventory map was shown the presence of past landslides in the study area by using Google Earth and remote sensing imageries. Total landslides were 368 in number, 30% (110) for testing purposes and 70% (258) for training purposes. The validation of Relative effect model was calculated with the Area under the curve such as the success rate curve and the prediction rate curve. This was adopted to check the validation and optimum landslide susceptibility zone categorization. The success rate curve of the model was 82.15% calculated whereas 82.73% was the predictive rate curve. According to the study, landslide susceptibility mapping was classified into four classes with 18.14% of the area being very high zone, 34.04% of the area being high zone, 30.26% area being moderately susceptible zone and 17.56% of the area being low susceptible to landslide occurrence zone. Hence, the results of this study highlight the spatial information of the area that may face landslide hazards and may be very helpful to planners, engineers, government agencies, stakeholders and other participants for the prevention, mitigation, management, and monitoring of landslide hazards and this model may also be applicable in other landslide areas.

Keywords: Landslide susceptibility mapping, Relative effect model, Remote sensing and GIS, Landslide causative factors, Neelum Valley

1. Introduction

Landslides are the type of natural destructive and geological calamities which are widely found in unequaled and steep terrain, having severe impacts on the economy and society [1, 2]. The rate of landslides is increasing with the contribution of other types of natural hazards such as rainfall, floods, snow, and earthquakes [3]. Unpredictable expansion and increasing population and urbanization of uneven topographic regions are the other anthropogenic factors to increase the landslides in developed and underdeveloped countries [4, 5]. Research and academic institutes and government agencies are working continuously on landslide occurrences to find out solutions for analyzing, predicting, and mitigating them [6].

Pakistan consists of the three largest northern mountain ranges named Himalaya, Karakoram, and Hindukush. The Himalayas is the most devastating and prone landslide range [7] having 30% of total landslides in the world [8]. It consists of rugged mountains, active tectonic activities, steep slopes, climatic conditions, deep weathering of strata, geology, and infrastructure on the unstable slope [2, 9, 10]. Seismic activities and monsoon rainfall are the primary triggering factors of landslides [4]. During the rainy season (monsoon season June to August), a massive amount of landslides are triggered due to the contribution of tectonic activities and geological properties in the Himalayasrange [10]. Approximately, more than 200 people

and 1 billion US Dollars in economic losses take place due to landslide hazards every year [11].

Neelum Valley is the largest district of Azad Kashmir and the part of the lesser Himalayan mountain where frequent landslides occur every year. The landslides are triggered due to various causative factors related to natural and human and trigger factors such as rainfall, tectonic movements, stream erosion, snowfall, and storm waves [12]. October 8, 2005, was a time when a very devastating hazard such as an earthquake with a 7.6 Mw magnitude triggered and approximately, 26,000 people died, directly and indirectly, millions of people lived without a home, and approximately, 5million US$ property was destroyed [13]. Every year landslides are affecting hundreds of people and approximately, one billion US$ of property is lost [14, 15]. The tendency of landslide occurrence has been listed from 1990 to 2005 and these trends will further increase in the future caused of human interference over the fracture and frail slopes [16]. Population growth takes place pressure on the fragile and weak slopes because of agriculture, infrastructure development, and habitation [10]. On the other side, the area of forest decreases, which produces more landslide risk [17, 18]. Seasonal and diurnal temperature and immature and young geology are other factors that help in the occurrence of landslides [18, 19].

Many scientific societies and communities have worked on landslide susceptibility in various regions of the

*Corresponding author: syed.sajjadmuhammad@uop.edu.pk

world [20, 21]. Landslide hazard mitigation and management studies are linked with landslide susceptibility mapping [10, 22]. The preparation of a Landslide susceptibility map is essential to understand the slope activities and their regulation components [4]. Landslide susceptibility mapping showed the target area into different zones according to the chance of landslide occurrence [23, 24]. Landslide inventory represents the extent of landslides, their types, and past and present landslide intensity in the target area [25, 26]. Landslide inventory, causative factors, and suitable methods have been used for the assessment of landslide susceptibility [27, 28].

Geospatial technology plays an effective role in landslide analysis. The use of geospatial techniques has been enhanced because of the statistical abilities, spatial information, and handling the large datasets [29, 30].

Various prediction methods such as qualitative, quantitative, direct, and indirect approaches have been utilized for assessing landslide susceptibility worldwide [31, 32]. The qualitative approaches such as heuristic and direct Geo-morphological mapping are based on personal knowledge and skills whereas the quantitative approaches are based on a numerical calculation between the landslides with their controlling factors [33, 34].

Hence, an effort has been made to create the landslide inventory map, select the suitable landslide causative factors and develop the landslide susceptibility map to show the landslide susceptibility areas by applying a GIS-based Relative Effect model. Relative Effect model is a bivariate statistical and quantitative approach, which provided the relationship between the causative factor with landslide events in the study area. The predictability and accuracy of the model were carried out through the success and prediction rate curves in landslide susceptibility modeling. The result of the study provides help to the government, private, academic, and research institutes, planners, and decision-makers to emphasize proper mitigation scales.

2. Material and Methods

2.1 Investigation site

Neelum Valley is the largest district and most beautiful place of Azad Kashmir having an attractive and resplendent spot for the tourist community (Fig. 1). It is located at longitude 73-75N and latitude 32-36E degree and situated toward the 20Km Northeast of Muzaffarabad city. Approximately, 3737Km^2 area is covered by lesser Himalayas with around 1.96 million population [35]. Himalaya George is called the area of Neelum Valley due to its rugged topography having lush green mountains, valleys, waterfalls, small terraces, and freshwater streams. The elevation of Neelum valley is between 980 meters and 6128 meters above sea level [36]. Sub-humid is the climate of Neelum Valley. Annual precipitation in Neelum Valley is 1650 mm [37].
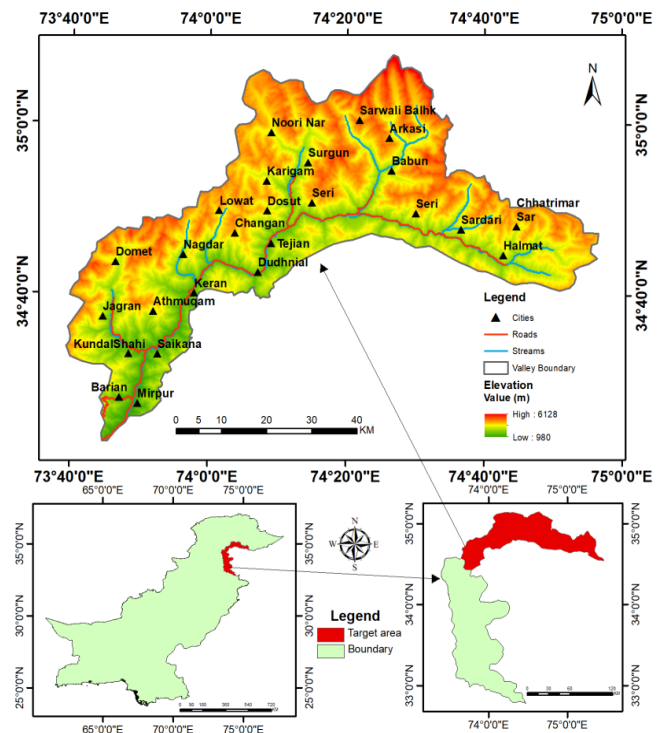

Fig.1: Study map of Neelum Valley.

2.2 Methodology

A database of various types of causative factors is developed which consists of topographic, hydrologic, and other related information derived from the sentinel 2 satellite images, geological maps, and digital elevation model (DEM) which determined the effect of landslides causative factors on landslide spatial arrangement (table 1). In the GIS environment, ArcGIS software was utilized for the preparation of landslide inventory and thematic maps of causative factors. The methodology of landslide susceptibility assessment is divided into three sections.

Table 1: Data used for landslide susceptibility model.

Factor maps	Data Acquisition	Scale/ Resolution	Methods
Landslide inventory	Field data and satellite images	1:50,000	Polygons and points
Lithology	Geological map	1:50,000	Polygons
Slope Gradient	ALOSPALSAR DEM	12.5m	Natural Break
Slope Aspect	ALOSPALSARDEM	12.5m	Natural Break
Elevation	ALOSPALSAR DEM	12.5m	Natural Break
General Curvature	ALOSPALSAR DEM	12.5m	Natural Break
Profile Curvature	ALOSPALSAR DEM	12.5m	Natural Break

Plan Curvature	ALOSPALSAR DEM	12.5m	Natural Break
TRI	ALOSPALSARDEM	12.5m	Natural Break
SPI	ALOSPALSAR DEM	12.5m	Natural Break
Distance from stream	ALOSPALSAR DEM	12.5m	200m interval
Drainage density	ALOSPALSAR DEM	12.5m	Natural Break
Distance from road	Topographic map	1:50,000	200m interval
NDVI	Sentinel 2	10 m	Natural Break
NDWI	Sentinel 2	10 m	Natural Break
Distance from faults	Geological maps	1:50000	200m interval
Land-use Land-cover	Sentinel 2	10m	classification
Rainfall (mm)	GPM	10m	Natural Break

2.3   Landslide inventory

First step was to prepare the past landslide inventory map. For this purpose, the landslide sites were collected through Google Earth and GPS in a detailed field investigation. Integrated the field information with the Sentinel satellite images at a spatial resolution of 10m is utilized for mapping and accuracy of landslides. Fig. 2 shows the diagnostic shapes of different types which define landslide classification using Varnes classification [38]. A total of 368 landslides have been identified. The digitized landslides were rasterized with the 12.5×12.5 m spatial resolution. This rasterized landslide inventory was used to calculate the number of grids in different classes of each causative factor for computing the ratio of landslide frequency. The landslide inventory database is randomly divided into subsets of 70% for training and 30% for testing.
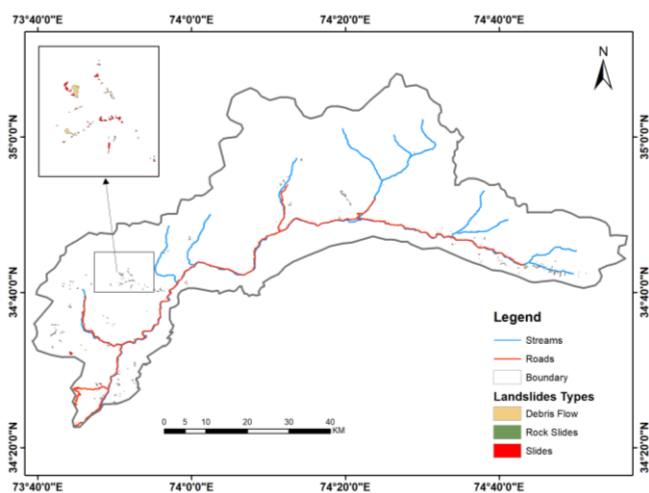

Fig. 2: Spatial distribution of various types of landslides in the study area.

2.4   Causative factors

After developing the landslide inventory map, Neelum Valley with 17 causative factors such as geology, distance from road, distance from stream, distance from fault, slope gradient, elevation, slope aspect, slope general curvature, profile curvature, stream power index, plan curvature, drainage density, terrain roughness index, NDVI, NDWI, LULC, and rainfall were selected for the landslide susceptibility assessment and mapping.

2.5   Geological map

Geology is an important factor and has a close relation with landslides [39]. The lithology and tectonic setting have a great impact on slope stability. It also affects the permeability and strength of soil and rocks. In Neelum Valley, landslides and surface geology have strong relations with each other. The surface geology of Neelum valley is mapped from the Geological map of Northern Pakistan which is acquired from the National Center of Excellence in Geology, University of Peshawar prepared by M.P. Searle and M. Asif Khan in 1996 (Fig. 3a) which contains such formations that is Murree formation (Nasueri group), Surgun group, Kundal Shahi group (Saikhala Series), and Nani group. These formations were different complex types of rocks (table 3).

2.6   Topographic parameters

ALOSPALSAR DEM having a 12.5-meter resolution was utilized to extract the topographic and hydrologic parameters. Topographical parameters extracted from DEM were slope gradient, slope aspect, elevation, general curvature, profile curvature, plan curvature, and terrain roughness index.

Slope gradient is the change of slope angle from general to steepest where the flow of water and movement of other materials moves toward slope direction. It plays also a vital role in the geomorphology and hydrology of the area. Rate of change of slope gradient describes the speed of surface and surface flows [40-42]. Therefore, frequency of landslide occurrence depends on the slope gradient. The slope map of Neelum Valley has been extracted from the ALOSPALSAR DEM having a 12.5-meter resolution, as shown in Fig. 3b. The slope map is classified into 0-18, 18-28, 28-38, 38-48, and 48-83 (table 3).

Dimension of the slope is described through the slope aspect. It has a great effect on landslide occurrences and has been utilized for landslide susceptibility mapping [34]. According to previous studies, the slope aspect has an indirect impact on landslide occurrences. Duration and sunlight intensity, rainfall, and soil moisture are the factors where the slope aspect depends on them. These factors have a great relation with landslides and vegetation cover [43]. The slope aspect factor has been extracted from ALOSPALSAR DEM as shown in Fig. 3c. There are nine dimensions such as flat, north, northeast, east, southeast, south, southwest, west, and northwest, and has been displayed in Fig. 3c, and Table 3.

Elevation is the topographic factor and has a significant role due to landslides taking place from up to downward direction [44]. It affects different geological and geomorphological conditions. Elevation differentiates maximum and minimum points within landscape [45]. ALOSPALSAR DEM with 12.5m resolution has been used to

extract the elevation factor as shown in Fig. 3d. Landslides occur due to the variation in elevation among the crown and toe caused by gravity which affects the whole system of terrain.

Curvature describes the morphology of topography with respect to changes in slope angle [46, 47]. It is also an important factor in landslide events where flow direction depends on the curvature of the landscape [24, 48]. Curvature was found in three sub-regions such as concave, convex, and flat. Concave area is positive values, convex consists of negative, and flat has zero value due to its nature. DEM was utilized to extract general curvature and classified it into five classes in this study as shown in Fig. 3e.

Profile curvature defines the vertical plan where it finds out the impact of topographical morphology on flow circulation. Profile curvature works on the changing angle of slope on flow path [49]. Profile curvature worked as opposed to plan curvature factor. It is divided into sub-regions such as concave, convex, and flat according to hill slope. ALOSPALSAR DEM was used to generate the profile curvature in the GIS environment as shown in Fig. 3f.

Plan curvature defines as the horizontal plane where it find-out the impact of topographical morphology on flow circulation. Plan curvature works on the convergence and divergence of water during that time when erosion takes place through flow of water on the surface [50-52]. Plan curvature was extracted from DEM as shown in Fig. 3g.

Terrain roughness index calculates the difference between the maximum and minimum height points in a total area [53]. It is an important morphometric causative factor that regulates slope stability. It shows the movements of the slope and plays an indirect role in landslide occurrence. TRI is calculated by using the following equation:

$$\text{Terrain Roughness Index } = \sqrt{|x|(\max^2 - \min^2)} \quad (1)$$

Whereas the max and min show the maximum and minimum values [54]. Terrain Roughness index was generated from ALOSPALSAR DEM as shown in Fig. 3n. It was categorized into five classes (table 3).

2.7   *Hydrological parameters*

Hydrological parameter is drainage density, stream power index, and rainfall.

Drainage density is a hydrological parameter. This parameter is calculated through the total length of stream or river divided by total area of the drainage basin. This parameter shows the runoff water from the channels. However, drainage density is the quantitative value. Higher value represents an increase in the runoff ratio of water. Higher drainage density value shows high possibility of landslide occurrence. The equation of drainage density is given below:

$$\text{DrainageDensity} = \frac{\text{Lk}}{\text{Ak}} \quad (2)$$

Whereas DD is drainage density, Lk is the total length of stream or river and Ak represents the total area of the drainage basin. The drainage density map of Neelum Valley was prepared from ALOSPALSAR DEM as shown in Fig.3j.

Stream power index is calculated as the erosion property of the stream in the flow accumulation area [55]. It describes the erosion power of the stream with the slope [56]. The higher value of stream power index shows the high probability of landslides due to the high possibility of erosion power. Stream power index is calculated by:

$$\text{Stream Power Index} = A \tan \beta/b \quad (3)$$

Whereas A represents the accumulated area and b is a slope (degree). ALOSPALSAR DEM was used to prepare the SPI map as shown in Fig. 3m. The SPI map was classified into five classes such as very low, low, moderate, high, and very high. The positive values of Relative Effect of each class of steam power index indicated high ratio of landslide found where negative values have no probability of landslide events.

2.8   *Rainfall map*

Rainfall is a very prominent and triggering factor in landslide occurrences [57]. Majority of landslides occurred due to the rainfall-triggering factor. Occurrence of landslides depends on the amount of rainfall as well as duration of rainfall so it can be said that landslides occurrence is directly proportional to the amount and duration of rainfall [58, 59]. It reduces the cohesion power of soil under saturation conditions [60]. Long-term duration of rainfall causes landslides in the study area. It produces surface runoff as well as discharge of unconsolidated ground material. Global precipitation measurement mission (GPM) data was utilized for the rainfall data of the study area. This rainfall data was used to prepare the rainfall map by using the IDW interpolation technique in GIS (Fig. 3q). The rainfall values were categorized into five classes (table 3).

2.9   *Environmental factors*

Environmental factors include NDVI, NDWI, and LULC

NDVI and NDWI

Satellite images such as Sentinel Images with 10-meter resolution were downloaded from the Sentinel Website. Sentinel Images were used to extract the NDVI and NDWI. Normalized difference vegetation index is a significant role in landslide occurrence and landslide susceptibility mapping [61]. The purpose of NDVI is to calculate the density of vegetation in form of forest, agriculture, range, cropland, etc., on the land surface [62-65]. The presence of dense vegetation decreases the landslide occurrence but absence of vegetation increases the rate of landslide events due to less cohesion power in soil. The NDVI is the difference between the red band and Infrared band of satellite images. The equation of NDVI is given below:

$$\text{NDVI} = \frac{\text{NIR}-\text{RED}}{\text{NIR}+\text{RED}} \quad (4)$$

Where NIR is the near-infrared band and RED represents the red band of satellite image. The range of NDVI is between -1 to +1. The +1 value represents highly concentrated and dense vegetation and -1 represents a low concentration of vegetation. Satellite image such as Sentinel 2 was used to prepare the NDVI image of the study area as shown in Fig. 3k. The NDVI map was classified into five classes.

McFeeters developed the Normalized difference water index in 1996 to determine the water body associated with wetlands [66]. The equation used for NDWI is given below:

$$NDWI = \frac{BAND\ GREEN - BAND\ NIR}{BAND\ GREEN + BAND\ NIR} \qquad (5)$$

The result of NDWI shows that the value greater than zero represents the water surface area and the value equal to or less than zero represents non-water surface area. This index is based on remote sensing satellite base image phenomenon. Sentinel 2 satellite image was used to prepare the index map of the study area as shown in Fig. 3l.

Landuse landcover map

Landuse is also a key factor in the modification of landuse patterns and consolidated slope material through human intervention and changes in the environment [67]. It also affects the hydrology of the area as well as the mechanical properties of the soil. Landuse factor is considered responsible for the evaluation of landslide susceptibility [68]. In hilly areas, road networks with infrastructure, etc., lead to a loss of the stability of slopes due to overburden and undercutting. Deforestation occurs due to the expansion of towns and villages which reduces the cohesion power provided by roots.

Generally, low land cover includes non-vegetated areas and bare land is more suspected that cause landslides prone [21]. A high land cover includes densely vegetated areas that strengthen the ground because dense vegetation is preventing erosion. Cultivation causes the incidences of landslides due to saturation of soil and removal of the surface soil layer. Sentinel 2 LULC image having 10m spatial resolution was downloaded from the ArcGIS website [69]. This image is prepared using maximum likelihood based on supervised classification. This image was used to clip the landuse landcover area of the study area. LULC map has eight LULC units of bare land, build area, clouds, crops, Rangeland, snow/ice, trees, and water (Fig. 3o) and the area of each unit was shown in table 3.

2.10 Proximity factors

Distance from Road, stream, and fault

Generally, Linear features including roads and streams decrease resisting force which leads to instability of slope and reduces the factor of safety [70, 71]. Faults are the breaks found in the tectonic features which decrease the strength of the slope. Thereby, distance from road, steam, and fault is linked with the possibility of landslides. River and road were digitized from topographic sheets of the study area. Faults map was prepared from the fault map of Neelum valley [72].

Distance from stream, road, and fault is calculated by using the multiple buffer tool in ArcGIS software. The distance from the road, stream, and fault also has a great effect on the landslide occurrence. This effect was examined by utilizing the Relative effect model for the assessment of landslide susceptibility. This tool created the five buffer zones with 200-meter intervals on the map as shown in Fig. 3(h, i, p). These distances were 0-200, 200-400, 400-600, 600-800, and > 800 meters.
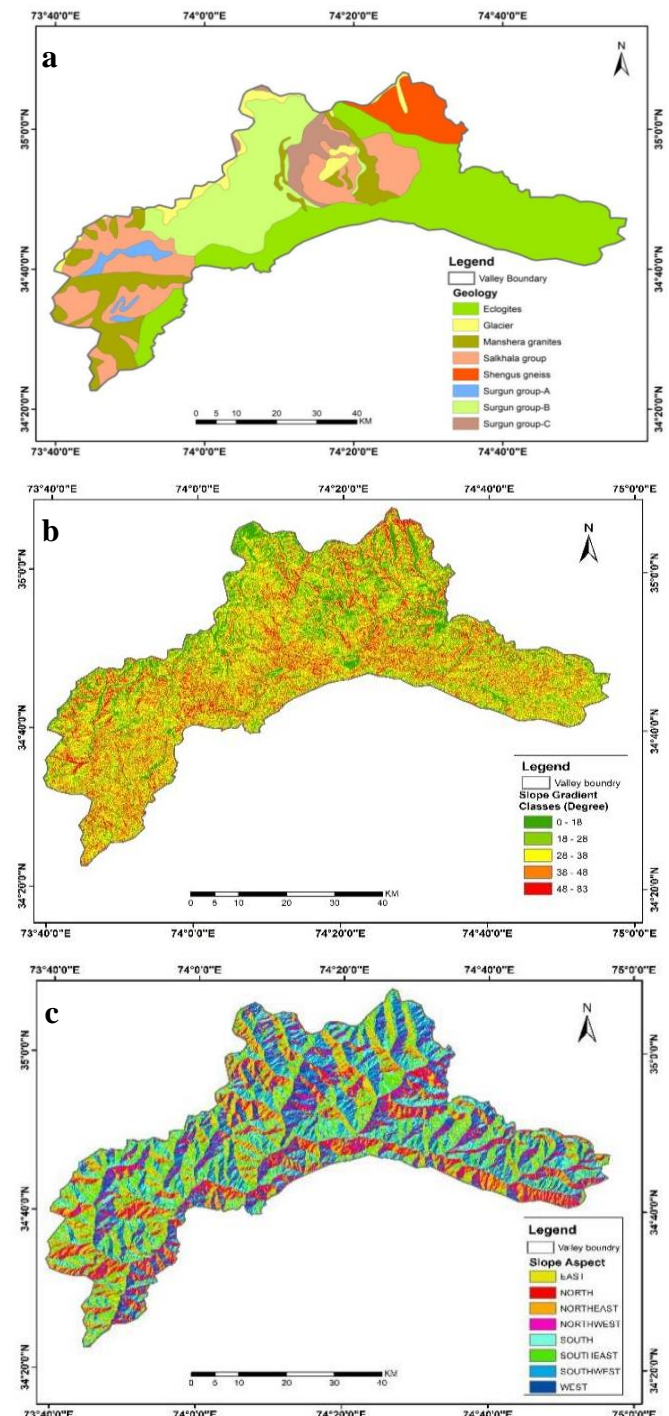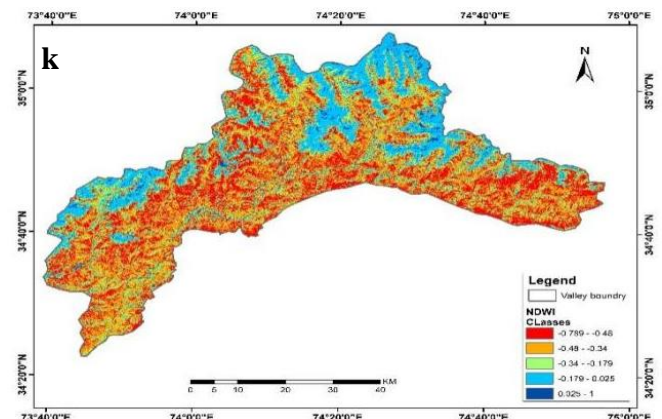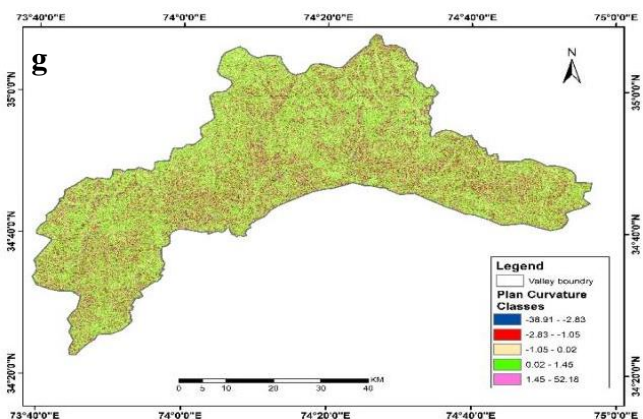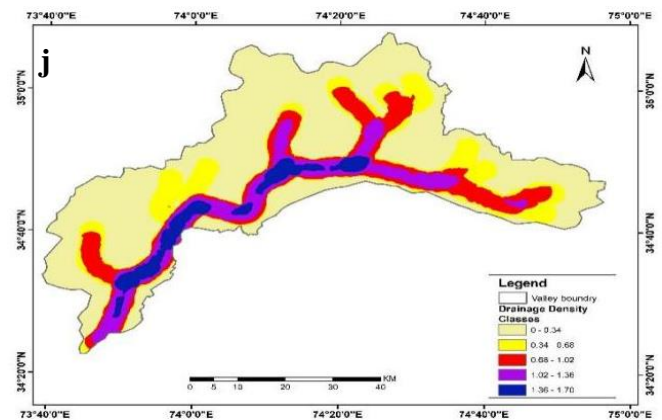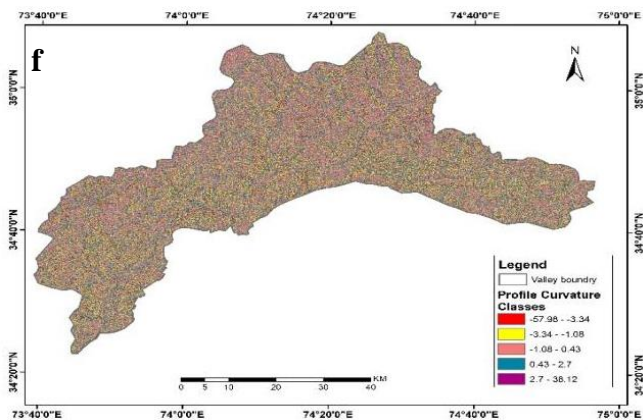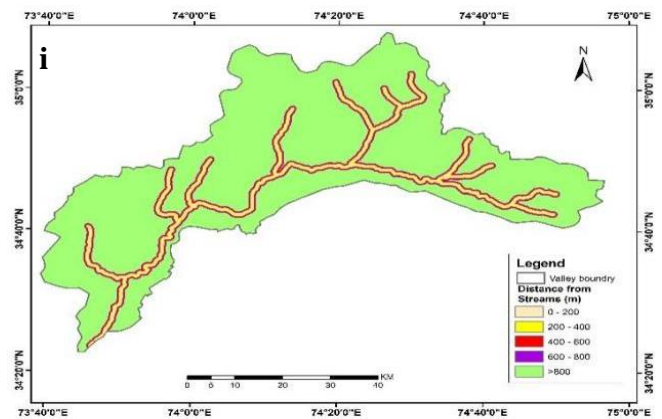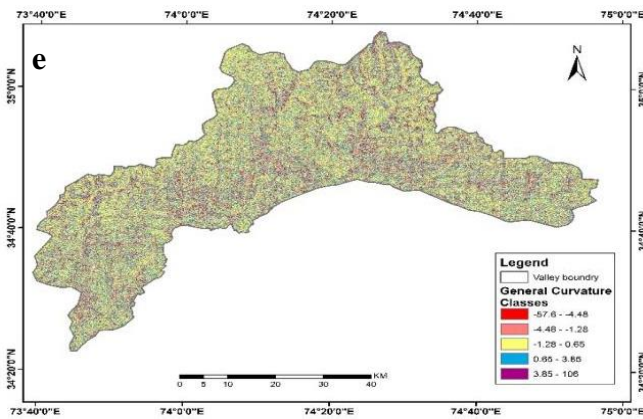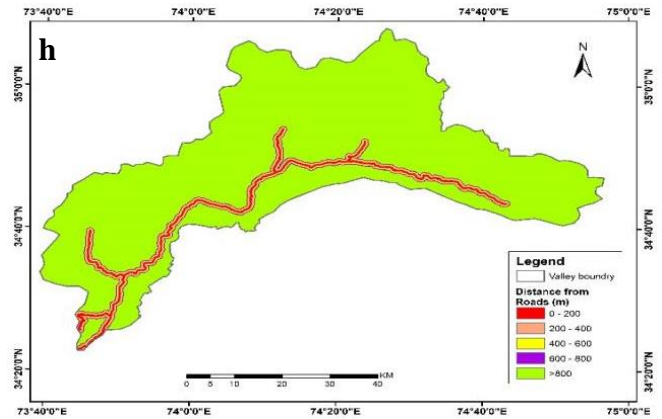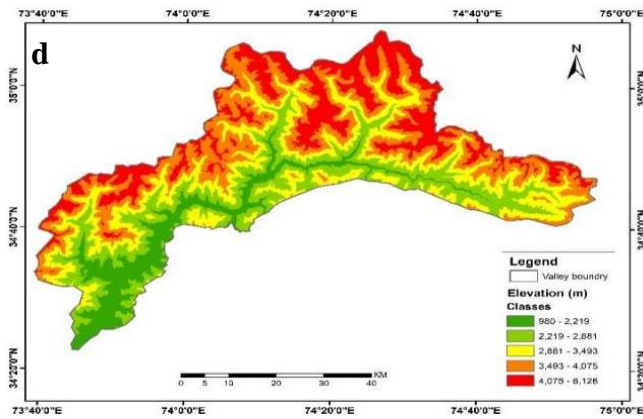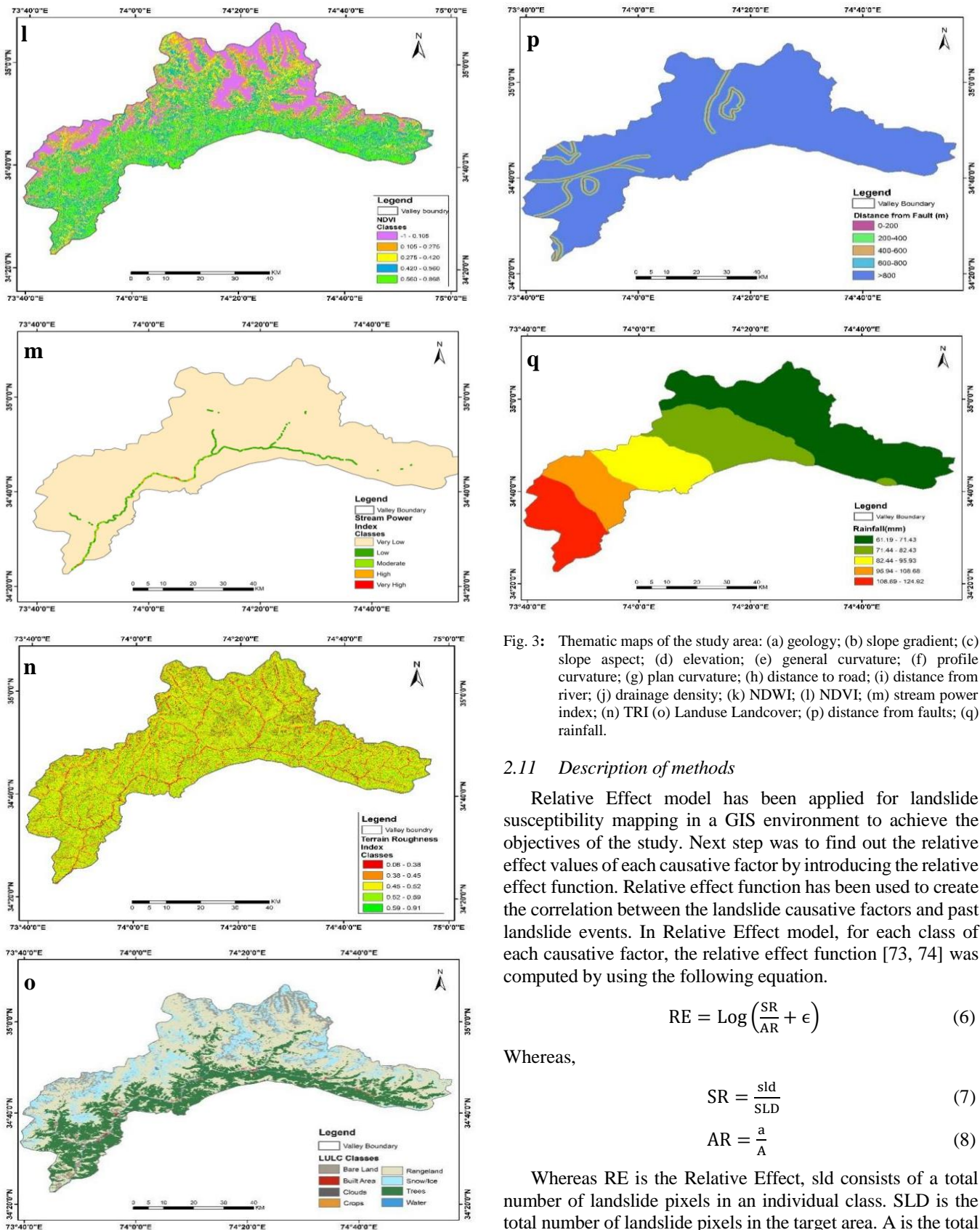
Fig. 3: Thematic maps of the study area: (a) geology; (b) slope gradient; (c) slope aspect; (d) elevation; (e) general curvature; (f) profile curvature; (g) plan curvature; (h) distance to road; (i) distance from river; (j) drainage density; (k) NDWI; (l) NDVI; (m) stream power index; (n) TRI (o) Landuse Landcover; (p) distance from faults; (q) rainfall.

2.11 Description of methods

Relative Effect model has been applied for landslide susceptibility mapping in a GIS environment to achieve the objectives of the study. Next step was to find out the relative effect values of each causative factor by introducing the relative effect function. Relative effect function has been used to create the correlation between the landslide causative factors and past landslide events. In Relative Effect model, for each class of each causative factor, the relative effect function [73, 74] was computed by using the following equation.

$$RE = Log\left(\frac{SR}{AR} + \epsilon\right) \qquad (6)$$

Whereas,

$$SR = \frac{sld}{SLD} \qquad (7)$$

$$AR = \frac{a}{A} \qquad (8)$$

Whereas RE is the Relative Effect, sld consists of a total number of landslide pixels in an individual class. SLD is the total number of landslide pixels in the target area. A is the total number of pixels in the target area and a contains the total number of pixels in an individual class. ε is a very small positive

value near zero. Relative Effect values of each class of 17 causative factors were calculated as shown in table 3.

2.12 Landslide susceptibility maps and validation

This logarithmic model gives the analysis of positive and negative quantitative effects. All the causative factors maps were integrated into the GIS environment to determine the landslide susceptibility index map. As a result, landslide susceptibility zones were developed on the bases of the Landslide susceptibility index. This algebraic summation equation is given as;

$$LSI = \sum RE \tag{9}$$

In this study, four landslide susceptibility zones have been developed from low to very high classes in Neelum Valley. The Relative Effect model base on the scale consists of positive and negative values. There are three cases found in the present relationship analysis [73, 74].

Effect of Negative values: when the value of Relative Effect scale is less than zero, the effect of probability of landslide susceptibility would be decreased.

Effect of Positive values: if the value of Relative Effect scale is greater than zero, the chances of a landslide would show high.

Effect of Zero value: the zero value of Relative Effect would show no effect on landslide susceptibility.

These values for each class of causative factor determined the relationship between the landslide sites and each class of causative factor map.

In third section, prediction and success curve rate were used to find out the validation and performance of relative effect model.

3. Result and Discussion.

Relative Effect model has been utilized in different areas of the world for landslide hazard mapping. In this article, the landslide susceptibility zone map of Neelum valley has been prepared by using Relative effect model which shows landslide-prone areas. These prone areas indicated the relationship between the causative factors and spatial distribution of past landslide inventory.

3.1 Landslide inventory of Neelum Valley

A Landslide inventory map shows the distribution of landslides in the Neelum valley separately. A Landslide inventory map is a primary step for the prediction of landslide susceptibility zonation but it is very difficult to take and map every landslide point because of time and tools availability. A total of 368 landslide sites were delimited, interpreted, and digitized on Sentinel-2 images. Field survey was conducted due to remove the uncertainty in the landslide inventory data and ground truth. Fig. 4 shows the different locations of landslides at different points. These landslides were classified into major types such as slides, debris flow, and rockfall according to Verne's classification. Among the landslides, 66.22% of landslides are slides, debris flows are the second occurring

phenomena which have 33.70%. Rockfall is found in the least amount and has 1.08% of landslides. During the field survey, majority of the landslide were recorded near the road and rivers. The smallest landslide is identified with an area of $0.0001km^2$ while largest landslide covered an area of $0.3236Km^2$. A total number of 368 landslides, slides were 240 in number and covers $3.4717 Km^2$ of the total landslide area. 124 landslides are the debris flow having $3.77km^2$ of total landslide area while rockfall contains 4 landslides and covers $0.05Km^2$ landslide area (table 2).

Table 2: Mapped landslide types, min/max area of landslides in the study area.

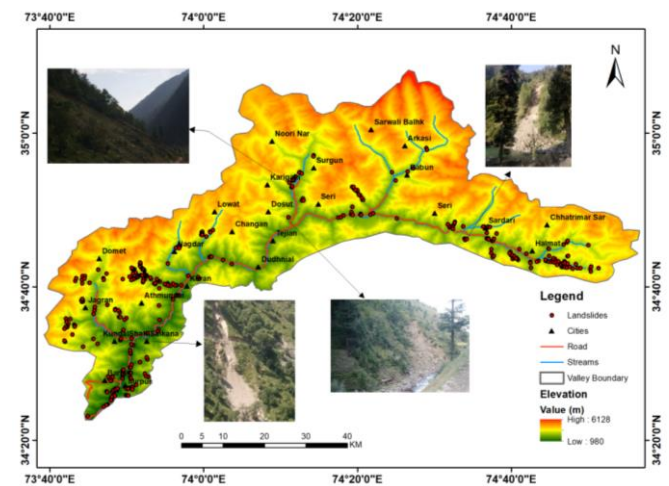| Landslides in Neelum Valley					
LS Types	LS	LS (%)	Min Area (Km^2)	Max Area (Km^2)	Average
Slide	240	65.22	0.0002	0.33	3.48
Debris Flow	124	33.70	0.0010	0.22	3.76
Rock Slide	4	1.08	0.0032	0.02	0.05
Total	368	100			

Fig. 4: Landslide inventory map of Neelum Valley.

3.2 Relationship between landslides occurrences and causative factors

Geology

The relation of landslide with the Lithological units through RE model shows that Tanawal formation, Manshera granite, Proterozoic (Kundalshahi group), and Paleozoic (Surguen Group-C) are high and positive relative effect values which represent high concentration of landslide occurrence. They have the RE value of 0.55, 0.25, 0.24, and 0.11 respectively (Fig. 5a, table 3). These classes of geology factor describe the weak structure and fragile types of rocks. The precipitation in uncovered forestation areas, deforestation, weak roots of trees, weathering, and frost action were also involved to increase weakness of geology of the study area. The lowest values -0.84 and -0.02 are calculated for the Surgun Group-B and Besal eclogites.

Slope gradient

The result showed that the rate of landslide occurrence increases where slope angle is above 38 degrees (Fig. 5b, table 3). In the slope gradient, positive RE values of 0.06 and 0.05 are calculated for 38-48 to 48-84 classes respectively. Fig. 5b represented a strong relationship between landslides and slope gradient with increasing the slope gradient of the entire area. This slope gradient shows the direct relation with the slope of the area and if weak and immature geology is found then the landslide ratio increases due to slope.

Slope aspect

It is observed that northwest to northeast and southward aspect shows high intensity of sunlight and precipitation which determined the high frequency of landslide events (table 3 and Fig. 5c). The lowest relative values were observed for east to southeast and southwest to west. North class has a high value of 0.31 RE thus highly susceptibility to landslide occurrences.

Elevation

The elevation from 980–2219 class shows a high value of Relative effect indicating the positive correlation between landslides and causative factors. The negative and lowest value of class (3493-4075) shows no landslide effect because the negative value gives no landslide effect and is less susceptible to landslide occurrences in the area. The result revealed that the rate of landslide events raised due to increasing the elevation as shown in Fig. 5d and table 2.

General curvature

Curvature is composed of flat, concave, and convex. The result of each class is shown in table 3 and Fig. 5e, that the concave region identified the high relative effect values in first and second class are 0.25 and 0.11, respectively. These values reflected the high ratio of landslide occurrence and show a strong relationship between the causative factors and landslides. A negative correlation was observed for flat and convex classes.

Profile curvature

Concave, convex, and flat are the classes of profile curvature. Profile curvature works opposite to general and plane curvature. A relative effect model was used to find out the effect of landslide events on profile curvature. The result showed that fifth class showed a high relative value (0.24). Fifth class identified the concave region which represented the highly susceptible and concentrated to landslide occurrence. The overall result is shown in Fig. 5f and table 3.

Plan curvature

Plan curvature has three sub-areas such as concave (positive), convex (negative), and flat (zero values). In this study, it is classified into five classes. The overall results revealed that concave region has a high value in relative effect model with the value of 0.23 and 0.15. a positive correlation was observed in concave class shows high susceptible to landslides (Fig. 5g and table 3).

Distance from the Road

The result shows that possibility of landslides decreases to move away from the roads as shown in buffers from 0 to 800 m. The positive values of distance from road are 0.58, 0.51, 0.43, and 0.33RE. They represent the high risk and susceptible to landslides and decrease the effect as move away (Fig. 5h and table 3). Expansion of roads, vibration due to high traffic volume, and removal of the material from the toe of mountains are the factors. These factors increase the rate of landslides and decrease due to decrease the effect of these factors.

Distance from the stream

The analysis revealed that distance from 0 to 800m shows a strong and positive correlation between the landslide and distance from the stream and the highest landslide possibilities. The results show that the highest value of Relative effect is to find out near the stream and decrease the values when increasing the distance from the steam which shows the landslide area is decreasing with increasing distance from the steam (Fig. 5i and table 3). The lowest RE value of -0.15 for the class of >800m distance from the stream.

Distance from faults

It is evident from table 2 and Fig. 4, that highest RE values 0.12 and 0.01 were calculated from the distance to fault class of 200-400 and >800m. The observed values are positive, representing the strong correlation of landslides with distance from fault and high probability of slope failure (Fig. 5p and table 3).

Drainage density

The drainage density classes of 0.34-0.68, 0.68-1.02, and 1.02-1.36 are indicating high RE values of 0.30, 0.34, and 0.04 respectively, and show a positive and strong correlation between landslides and drainage density. The lowest and negative RE value of -0.18 and -0.38 was calculated for class 0-0.34 and 1.36-1.7 and thus had less influence on landslide occurrence and landslide tendency (Fig. 5j and table 3).

Normalized Difference Vegetation Index

It is observed that the concentration of landslide occurrence is high in class 0.10–0.27 with a value of 0.42 due to less concentration of vegetation or deforestation which indicates positive and strong correlation between the landslides and NDVI whereas 0.42-0.56 class with the value of high concentration of vegetation indicates less rate of landslide occurrence and thus less prone to landslides (Fig. 5k and table 3).

NDWI

According to this index, the highest positive Relative Effect value of 0.38 and 0.01 is observed for -0.34 - -0.179 and -0.48- -0.34 classes respectively. They indicated a high rate of landslide tendency which represented a strong correlation between landslides and NDWI and highly prone to landslides. The lowest and negative values of -0.58, -0.09, and -0.31 indicate a weak relationship between NDWI and landslides and have a low rate of landslide tendency (Fig. 5l and table 3).

Stream power index

In the stream power index, the third and fourth classes show positive relative effect values as compared to the other classes which revealed a high probability of landslide occurrence as shown in Fig. 5m and table 3.

Terrain Roughness index

The results showed that the positive value of 0.33 and 0.77RE is calculated for 0.08–0.38 and 0.38-0.45 classes respectively. These high relative effect values indicated high ratio of landslide occurrence in the study area and showed strong and positive relation between landslides and TRI as compared to other classes (Fig. 5n and table 3).

Landuse landcover

In case of landuse landcover, mostly all the classes have positive values and indicate strong correlation between landslides and landuse landcover. The highest positive values of 0.82 and 0.65 are observed for crops followed by water. The snow/ice class is observed negative value of -1.38 indicating less susceptible to landslides (Fig. 5o and table 3).

Rainfall

Rainfall is responsible for the majority of landslides and is directly proportional to the amount of rainfall. The calculated values for rainfall classes 95.94-108.68 and 108.69-124.92 are highest with positive values of 0.09 and 0.44. The results show that the probability of a landslide is increasing as the rainfall increases and is highly prone to landslides. While the lowest and negative values of other classes show less susceptible to landslides and a weak correlation between them (Fig. 5q and table 3).

Table 3:   Neelum valley, relative effect values of the landslide conditioning parameters.

| CAUSATIVE FACTOR	CLASS	% OF PIXELS IN CLASS	% OF LANDSLIDE PIXELS IN CLASS	RE
GEOLOGY	Glacier	4.08	0	0
	shengus gensis	5.87	0	0
	Besal eclogites	35.92	34.53	-0.02
	Manshera granites	11.39	20.29	0.25
	Proterozoic (Kundalshahi group)	18.34	31.69	0.24
	Mesozoic (Surguen group-B)	19.24	2.81	-0.84
	Paleozoic (Surguen group-C)	3.38	4.35	0.11
	Cambrian(Tanawal formation-Surguen A)	1.78	6.34	0.55
SLOPE GRADIENT	0 - 17	12.32	8.26	-0.17
	17 - 28	24.81	22.60	-0.04
	28 - 38	31.21	33.09	0.03
	38 - 48	22.78	25.99	0.06
	48 - 84	8.89	10.05	0.05
SLOPE ASPECT	North	9.93	14.19	0.31
	Northeast	10.61	11.77	0.05
	East	12.40	10.96	-0.05
	Southeast	15.46	15.21	-0.01
	South	14.87	15.97	0.03
	Southwest	14.71	13.52	-0.04
	West	11.94	7.63	-0.19
	Northwest	10.07	10.74	0.03
DISTANCE FROM ROAD	0 - 200	2.30	8.71	0.58
	200 - 400	2.17	7.00	0.51
	400 - 600	2.08	5.64	0.43
	600 - 800	2.03	4.33	0.33
	>800	91.43	74.32	-0.09
DISTANCE FROM STREAM	0 - 200	3.72	16.81	0.65
	200 - 400	3.63	8.13	0.35
	400 - 600	3.53	7.77	0.34
	600 - 800	3.51	7.36	0.32
	>800	85.61	59.93	-0.15
GENERAL CURVATURE	-54.64 - -4.48	3.04	5.35	0.25
	-4.48 - -1.28	25.87	33.17	0.11
	-1.28 - 0.65	42.65	37.70	-0.05
	0.65 - 3.85	25.26	20.62	-0.09
	3.85 - 106	3.19	3.16	-0.00
ELEVATION	980 - 2219	10.65	31.06	0.46
	2219 - 2881	20.46	51.23	0.40
	2881 - 3493	22.92	17.18	-0.13
	3493 - 4075	26.22	0.53	-1.70
	4075 - 6128	19.75	0.00	0
PLAN CURVATURE	-38.90 - -2.83	1.69	2.90	0.23
	-2.83 - -1.04	13.20	18.83	0.15
	-1.04 - 0.03	38.27	37.85	0.00
	0.03 - 1.45	38.17	32.74	-0.07
	1.45 - 52.18	8.66	7.69	-0.05
PROFILE CURVATURE	-57.98 - -3.34	1.75	1.98	0.05
	-3.34 - -1.07	14.09	13.11	-0.03
	-1.07 - 0.43	49.16	42.11	-0.07
	0.43 - 2.7	32.04	37.59	0.07
	2.7 - 38.12	2.96	5.22	0.25
TERRAIN ROUGHNESS INDEX	0.08 - 0.38	6.48	13.94	0.33
	0.38 - 0.45	20.80	24.46	0.07
	0.45 - 0.51	36.91	33.10	-0.05
	0.51 - 0.59	27.07	22.72	-0.08
	0.59 - 0.90	8.74	5.77	-0.18
NDVI	-1 - 0.10	17.93	8.58	-0.32
	0.10 - 0.27	12.20	31.79	0.42
	0.27 - 0.42	18.72	29.60	0.20
	0.42 - 0.56	27.47	20.54	-0.13
	0.56 - 0.87	23.69	9.50	-0.40
NDWI	-0.78 - -0.48	27.28	7.12	-0.58
	-0.48 - -0.34	32.81	33.89	0.01
	-0.34 - -0.17	17.21	41.50	0.38
	-0.17 - .02	20.25	16.29	-0.09
	0.02 - 1	2.44	1.20	-0.31
DRAINAGE DENSITY	0 - 0.34	72.59	48.21	-0.18
	0.34 - 0.68	13.03	26.11	0.30
	0.68 - 1.02	9.54	20.75	0.34
	1.02 - 1.36	4.38	4.74	0.04
	1.36 - 1.7	0.46	0.20	-0.38
STREAM POWER INDEX	0 - 162747343	99.97	99.96	-0.0005
	162747343 - 623864818	0.02	0.01	-0-00001
	623864818 - 1329103309	0.01	0.01	0-0001
	1329103309 - 2875203075	0.00	0.02	0-0000001
	2875203075 - 6916762112	0.00	0.00	0
LANDUSE LANDCOVER	Bare Land	8.90	10.83	0.08
	Built Area	0.23	0.32	0.14
	Clouds	0.00	0	0
	Crops	0.16	1.06	0.82
	Rangeland	45.35	49.54	0.04
	Snow/Ice	15.62	0.66	-1.38
	Trees	29.02	34.45	0.07
	Water	0.70	3.10	0.65
DISTANCE FROM FAULTS	0 - 200	2.01	0.51	-0.59
	200 - 400	2.01	2.62	0.12
	400 - 600	1.99	1.32	-0.18
	600 - 800	1.94	0.83	-0.37
	>800	92.04	94.69	0.01
RAINFALL	61.19 - 71.43	41.30	29.62	-0.14
	71.44 - 82.43	20.25	15.29	-0.12
	82.44 - 95.93	13.88	3.98	-0.54
	95.94 - 108.68	11.08	13.69	0.09
	108.69 - 124.92	13.46	37.40	0.44
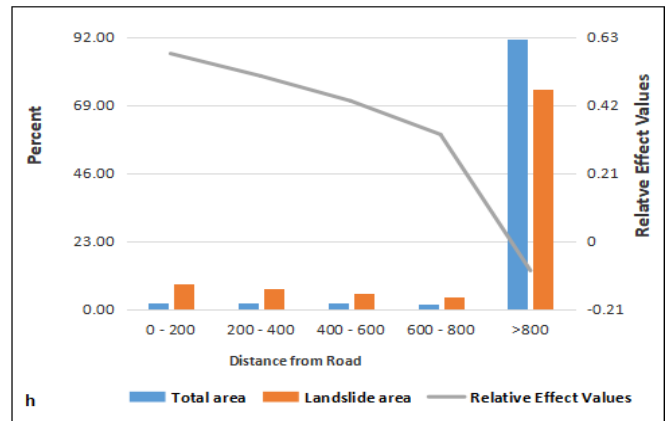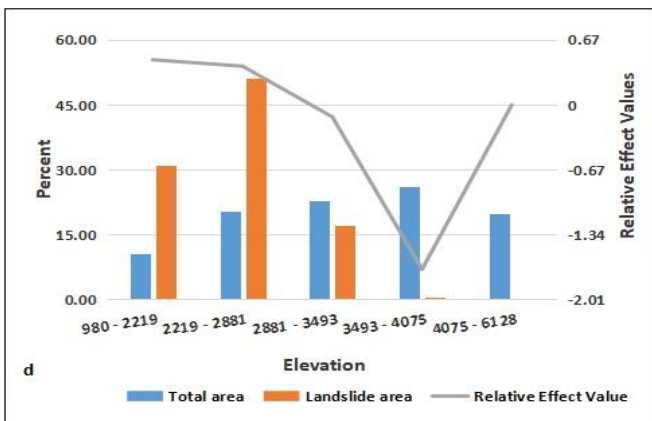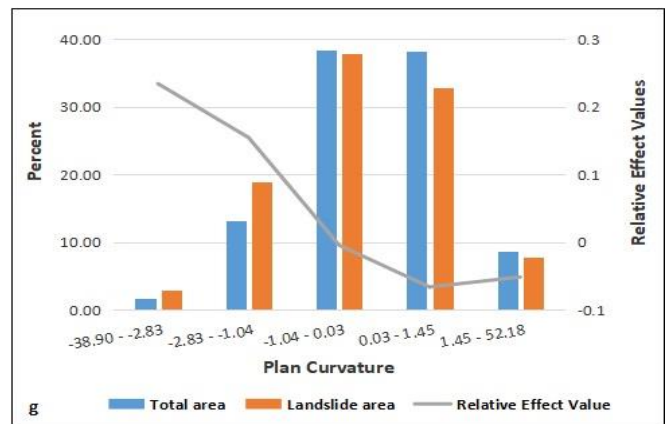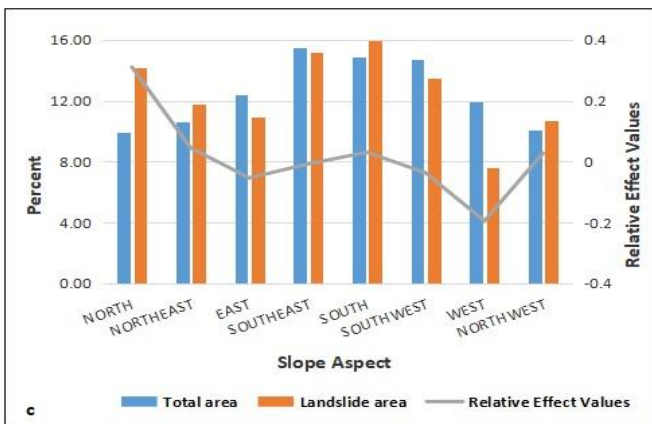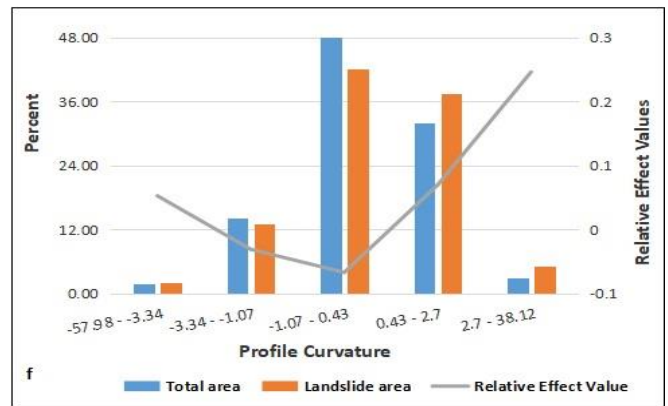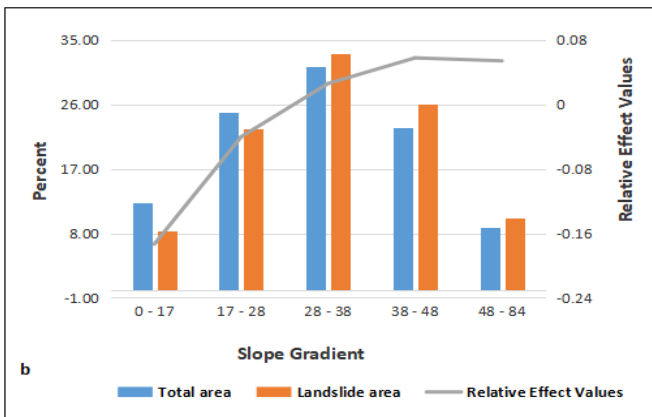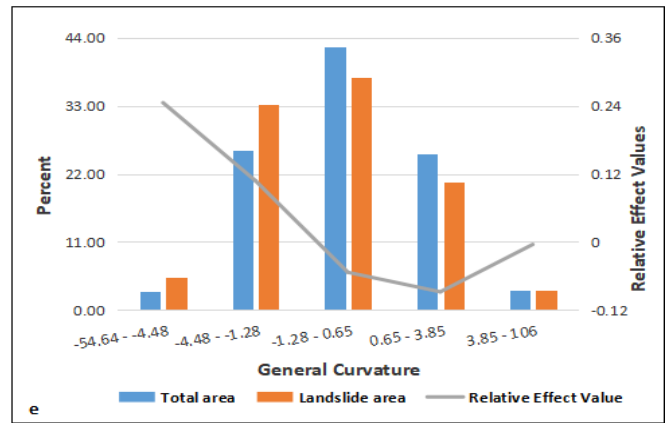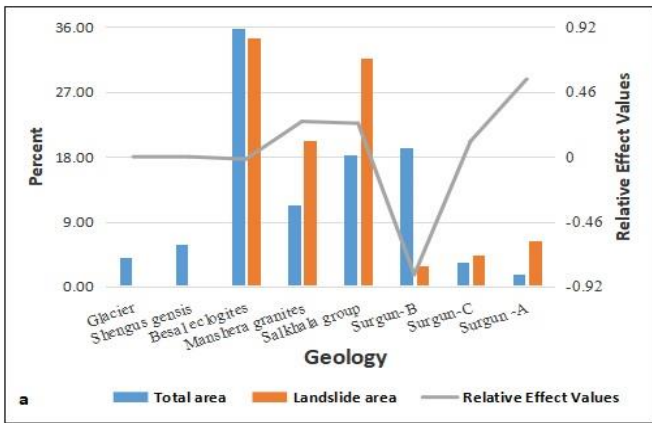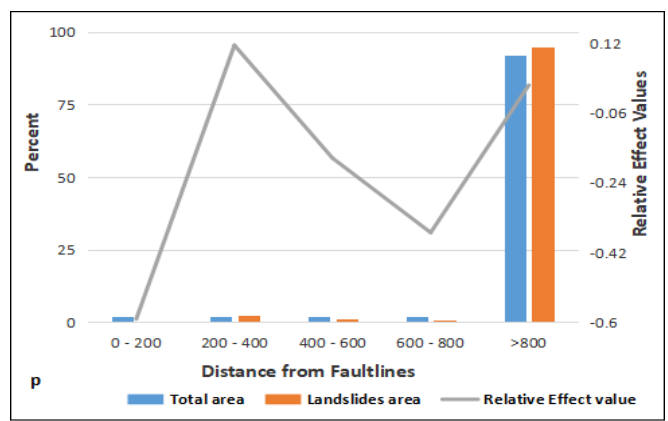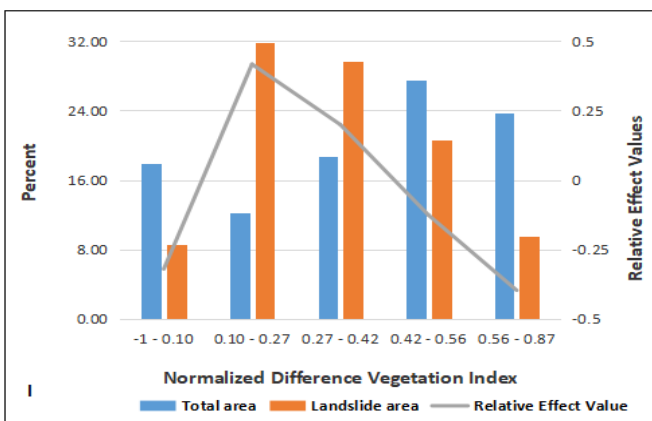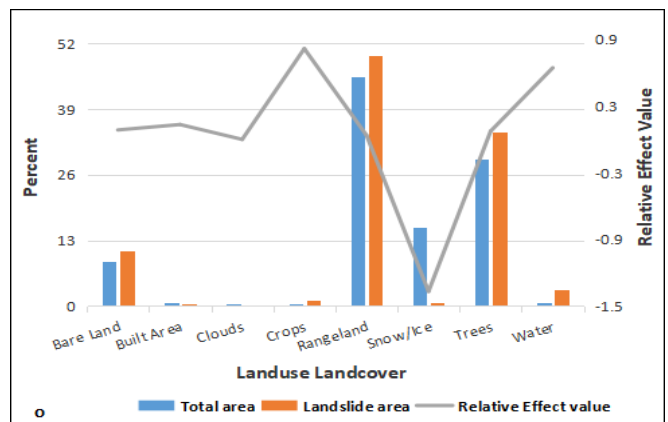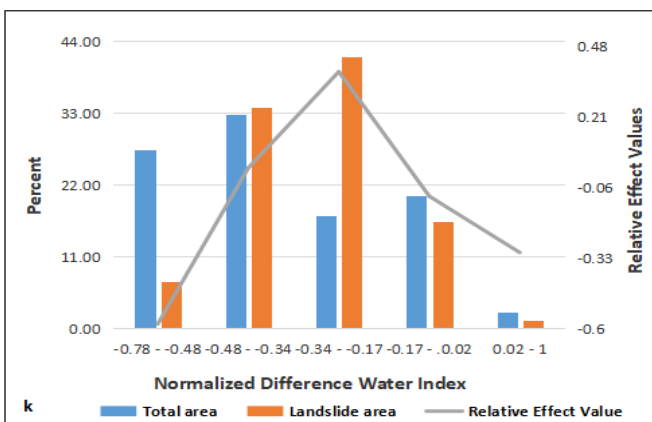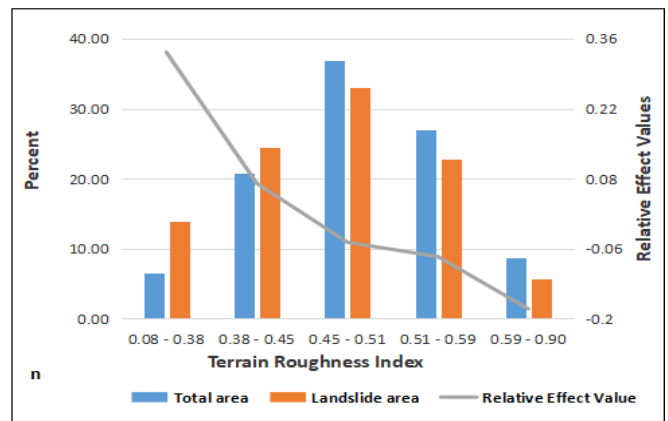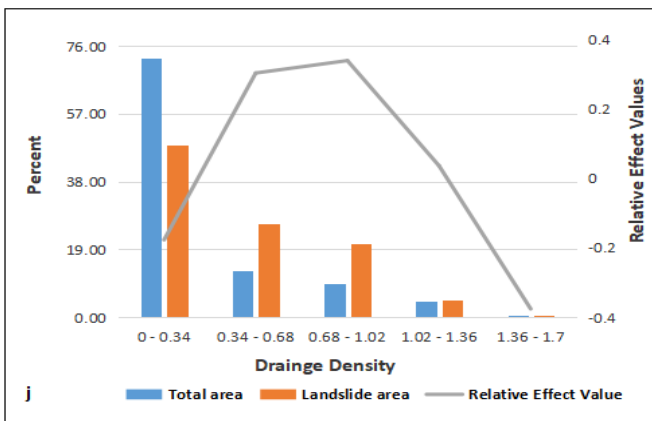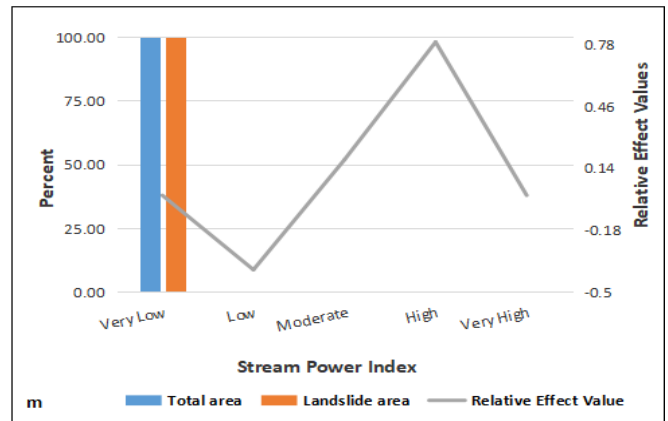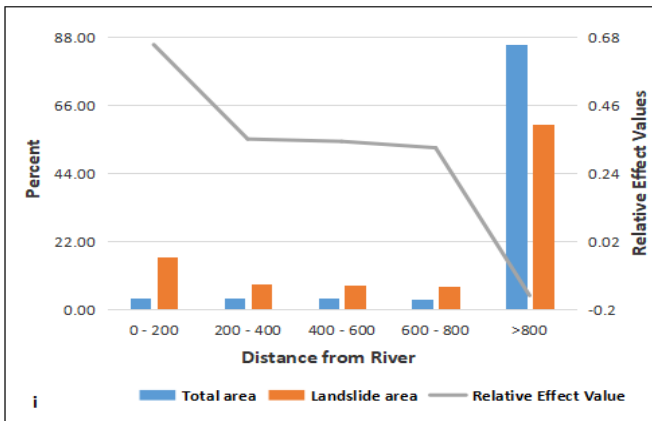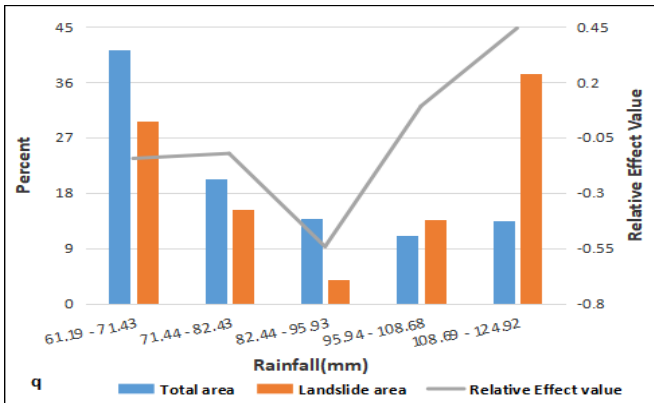
Fig. 5: Thematic maps of the study area: (a) geology; (b) slope gradient; (c) slope aspect; (d) elevation; (e) general curvature; (f) profile curvature; (g) plan curvature; (h) distance to road; (i) distance from river; (j) drainage density; (k) NDWI; (l) NDVI; (m) stream power index; (n) TRI (o) Landuse Landcover; (p) distance from faults; (q) rainfall

3.3 Landslide susceptibility zonation (LSZ)

In the GIS environment, 17 landslide causative factors were integrated with their relative effect values (table 2) to develop the landslide susceptibility index map of Neelum Valley (Equation. 9). The range of susceptibility was (-6.68 – 4.88) in the landslide susceptibility index map. Higher susceptibility values indicated a high rate of concentration of landslide occurrence in future. Landslide susceptibility index map was classified into four susceptibility classes by using the natural break method to prepare the landslide susceptibility map and to identify the level of prone areas based on the selected factors. These four classes are low, moderate, high and very high (Fig. 6). 15.50 % of the area was analyzed as the very high susceptibility zone and 33.75% was considered in the high zone of landslide susceptibility. The moderate landslide susceptibility class is 30.26% and low landslide susceptibility class is 17.56% of the entire area. The results showed that a total of 48.80% of the area was considered into very high and high susceptibility zones which make happen enormous damage in future (Fig. 6 and table 3). River and roadsides of the valley, infrastructure, and agriculture on fragile slopes are considered into very high landslide susceptibility zone. Fig. 7 further describes that the
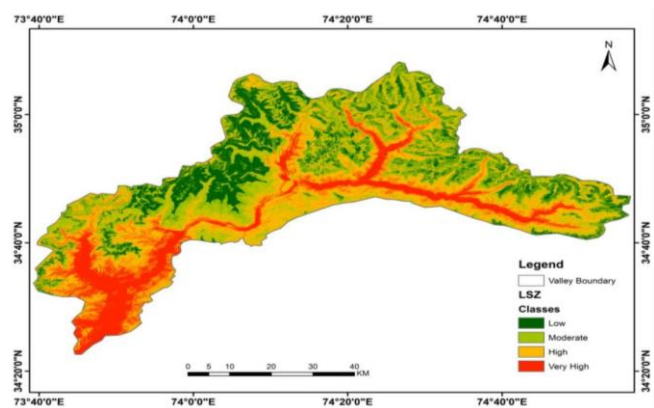

Fig. 6   Landslide susceptibility zones map Neelum Valley.

low susceptibility class has low landslides. The percentage of landslide area in moderate and very high susceptibility classes is comparatively more whereas, high susceptibility class is a high percentage of landslide area as compared to the other three classes.
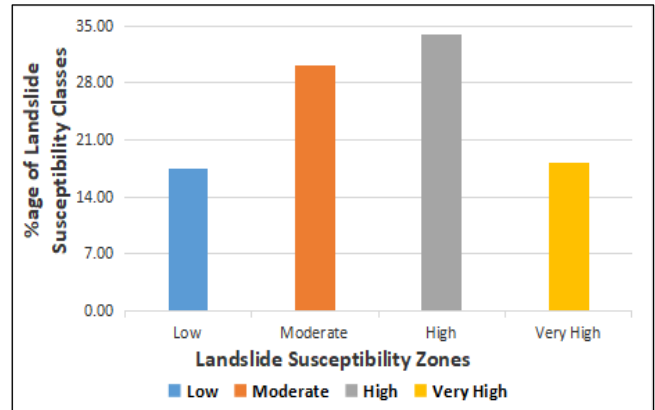

Fig. 7:   Landslide Susceptibility zones of Neelum Valley.

Table 3:   Landslide susceptibility zone of Neelum Valley.

Classes	Low	Moderate	High	Very High
Percentage	17.56	30.26	34.04	18.14

3.4 Validation and model performance

Relative Effect model has been used by generating the landslide susceptibility zone of Neelum Valley. The success and prediction rate curves were used to measure the accuracy of Relative Effect model for selected causative factors. The success rate curve was obtained by comparing the training data set (70%) of landslide inventory with the landslide susceptibility map. The prediction rate curve was plotted between the testing data set (30%) of landslide inventory which is used as validation data, with landslide susceptibility maps. These curves were calculated by dividing the landslide susceptibility index values into 100 classes and then combined with the past landslide inventory map. The resultant map indicated that existing landslide areas were falling in every susceptibility class. The success and prediction rate curves were built by mapping the landslide susceptibility index on the x-axis and cumulative percentage of landslide occurrence on the y-axis (Fig. 8). Both rate curves show the meaningful output of Relative Effect model and productive output of landslide susceptibility zone map. The traditional academic point system is used to classify the AUC into the following ranks for accuracy of models [75, 76] i.e. excellent (90-100%), good (80–90%), fair (70–80%), poor (60–70), and fail (50–60%). The qualitative analysis of the AUC of success and predictive rate curve of landslide susceptibility index map was 82.15% and 82.73% accuracy. AUC rate curves were found in the good category. Hence, it was found from the analysis that the Relative Effect model gives satisfactory results in Neelum Valley.
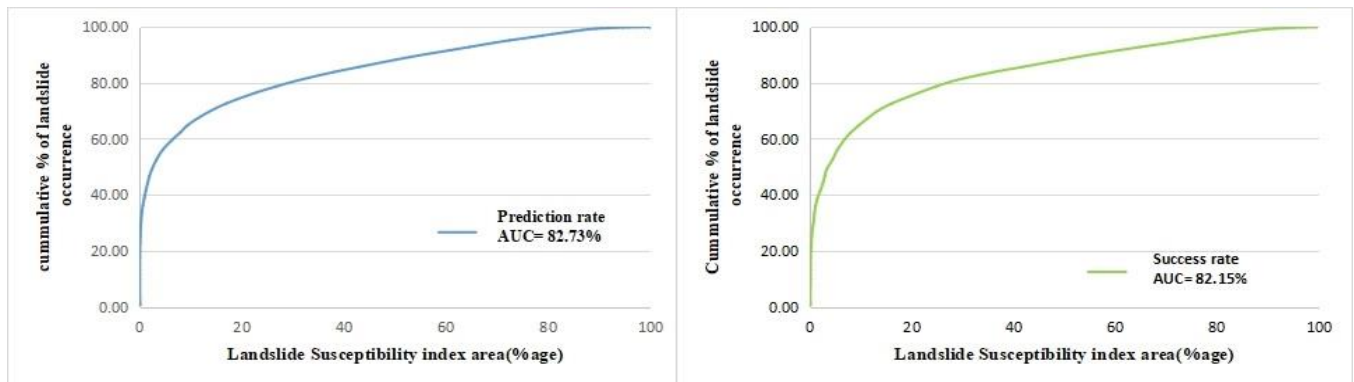
Fig. 8:   Success rate and predictive rate of the landslide susceptibility map.

3.5   *Discussion*

Every year, many human deaths and damage to their properties occur due to tremendous landslides. Therefore, a piece of comprehensive knowledge is required to understand and handle this phenomenon. Identifying past and new landslides that occurred in regions is essential to avoid future landslides. Various methods and approaches may be used to predict the landslide susceptible areas geographically. Relative effect model was used in this study to generate a landslide susceptibility map and to evaluate the relationship between the landslides and causative factors. In this study, a detailed landslide inventory map was prepared which is classified into three types of landslides included slide, debris flow, and rockfall. These types of landslides were examined during the field survey. 240 slide types of landslides were calculated having 65.22% of total landslides whereas debris flow consists of 124 landslides and has 33.70% of total landslides. Debris flow as compared to slide type covered a large area.

A developed database is comprised of landslide inventory and 17 landslide causative factors. Possibility of landslide occurrences depends on the calculated values of each class of causative factors that represent a high and low class of probability. These landslide causative factors were integrated into the GIS environment to develop the landslide susceptibility map. In this study, various significant causative factors such as terrain roughness index, drainage density, plan curvature, profile curvature, general curvature, geology, land-use landcover, stream power index distance from stream and road, were observed by using the relative effect model and show a strong correlation with the landslides of the entire area. In case of geology of the study area, the Surgun group A, Manshera Granites and Salkhala formation show high susceptibility to landslides due to unconsolidated material on the slopes, highly fractured and deformed. A total of 58.72% of landslide area was observed in these geological units. Slope greater than 29 degree indicates a positive and strong correlation between the landslide and slope gradient and increase the landslide ratio with an increase in slope gradient. The slope aspect from northwest to northeast and south aspect show more prone to landslides due to the long duration of radiation of sun and frost action due to the temperature variation and covered 53% of the total landslide area. Among the surface aspects, east to southeast and west to southwest got a negative correlation with the landslides. Distance from the road and stream from 0 to 800m are more concentrated and prone to landslides but the relationship between causative factors and landslides decreases with increasing the distance from road and stream. Distribution of landslides was more escalated within 200-400m and >800m from faults. The analysis reveals that Elevation from 980 to 2881m indicates a positive and strong correlation with landslides. Most of the area is found near the Neelum river and road and infrastructure development. In case of general, plan and profile curvatures, it is observed that concave curvature indicates a positive and strong correlation with landslides. Landuse landcover classes such as built area, crops, bare land, water, and Rangeland are more and highly susceptible to landslides. Terrain roughness index of 0.08 to 0.45 indicates a high erosion process which increases the rate of landslides and is thus prone to landslides. SPI is related to the erosion power of runoff water around the area. High rate of runoff water shows in the fourth and fifth class which represents high possibility of landslides. Drainage density is also a hydrological factor found to have high susceptibility in the 0.34 to 1.36 class of drainage density. In NDWI factor, -0.34 to 0.17 class is more prone to landslides and shows a strong correlation with landslides. NDVI shows a high value from 0.10 to 0.42 which describes the high probability of landslides occurrences. Range of the rainfall from 95.94 to 124.92 mm shows positive values of relative effect model which covered 51.09% of total landslide area. High rainfall classes included less vegetation with anthropogenic activities which increase the concentration of landslides.

The traditional academic point system is used to classify the AUC into the following ranks for accuracy of models [75, 76] i.e. excellent (90-100%), good (80–90%), fair (70–80%), poor (60-70), and fail (50–60%). Accuracy assessment of the model found in the good class of AUC as per traditional academic point system. The success and prediction power of model is 82.15% and 82.73% which is considered accurate and will suggest future research.

4.   Conclusions

Landslide susceptibility mapping is a primary and significant role to determine the landslide-affected areas in mountain regions. A comprehensive study is required to

understand and resolve the landslide phenomenon. Identification of the spatial probability of landslide-prone areas was the objective of this study by using the Relative Effect model. The hundred sixty-eight (368) landslide areas were digitized in the landslide inventory map. 17 causative factors such as slope gradient, slope aspect, elevation, terrain roughness index, general curvature, profile curvature, plan curvature, drainage density, stream power index, distance from river, distance from road, distance from faults, geology, rainfall, landuse landcover NDVI, and NDWI were integrated to prepared the landslide susceptibility map. Every causative factor was an important role to find out the effect of occurrence and non-occurrence of landslides with the help of Relative effect value. The negative values showed non-landslide occurrence and the positive value indicated occurrence of landslide.

Landslide susceptibility zonation map is classified into four classes such as low, moderated, high, and very high. The result showed that 15.05% and 33.75% were considered very high and high categories of landslide susceptibility. The analysis showed that the success rate curve was 82.15% and the prediction rate was 82.73% for landslide susceptibility mapping. Overall finding of this study shows the good performance of the model in landslide susceptibility assessment and will help the new research, planner, and developer for better planning and management of damage to infrastructure and identify future landslide-prone areas in the study area. The developed map can also be used for hazard and risk assessment of landslides. It is suggested to carry out this model in similar studies in other landslide-prone areas.

Acknowledgment.

Conflict of Interest.

Author(s) declare that the publication of this article has no conflict of interest

References

[1] S. Das, S. Sarkar, and D. Prasanna, "GIS-based landslide susceptibility zonation mapping using the analytic hierarchy process (AHP) method in parts of Kalimpong Region of Darjeeling Himalaya", Environmental Monitoring and Assessment, vol. 194, no. 3, pp. 1-28, 2022.

[2] R.M. Tayyib, M. Basharat, N. Hameed, M. Shafique, and J. Luo, "A data-driven approach to landslide-susceptibility mapping in mountainous terrain: a case study from the Northwest Himalayas, Pakistan", Natural Hazards Review, vol.19, no.4, 05018007, 2018.

[3] García-Rodríguez, M. José, J.A. Malpica, B. Benito, and M. Díaz, "Susceptibility assessment of earthquake-triggered landslides in El Salvador using logistic regression", Geomorphology, vol.95, pp.172–191, 2008.

[4] L. Bopche, P.P. Rege, and R.D. Joshi, "Landslide susceptibility mapping: an integrated approach using knowledge-based numerical rating scheme, remote sensing, and multiple overlay analysis", Journal of Applied Remote Sensing, vol.16, no.1, pp. 014503, 2022.

[5] M. Yawen, "Regional Scale Multi-Hazard Susceptibility Assessment: a case study in Mtskheta-Mtianeti, Georgia", University of Twente Faculty of Geo-Information and Earth Observation (ITC). 2011.

[6] J. Pankaj, and C.J. van Westen, "Use of quantitative landslide hazard and risk information for local disaster risk reduction along a transportation corridor: a case study from Nilgiri district, India", Natural hazards, vol.65, no.1, pp. 887-913, 2013.

[7] R.P. Gupta and B.C. Joshi, "Landslide hazard zoning using the GIS approach-a case study from the Ramganga catchment, Himalayas", Engineering Geology, vol. 28, no.1-2, pp. 119-131, 1990.

[8] T.H. Tran, N.D. Dam, F.E. Jalal, and N. Al-Ansari "GIS-based soft computing models for landslide susceptibility mapping: A case study of Pithoragarh district, Uttarakhand state, India", Mathematical Problems in Engineering, 2021.

[9] U. Kamp, L.A. Owen, B.J. Growley, and G.A. Khattak, "Back analysis of landslide susceptibility zonation mapping for the 2005 Kashmir earthquake: an assessment of the reliability of susceptibility zoning maps", Natural hazards, vol. 54, no. 1, pp. 1-25, 2010.

[10] U. Sur, P. Singh, and S.R. Meena, "Landslide susceptibility assessment in a lesser Himalayan road corridor (India) applying fuzzy AHP technique and earth-observation data", Geomatics, Natural Hazards, and Risk, vol. 11, no.1, pp. 2176-2209, 2020.

[11] D.P. Kanungo, M.K. Arora, R.P. Gupta, and S. Sarkar, "Landslide risk assessment using concepts of danger pixels and fuzzy set theory in Darjeeling Himalayas", Landslides, vol. 5, no. 4, pp. 407-416, 2008.

[12] F.C. Dai, C.F. Lee and Y.Y. Ngai, "Landslide risk assessment and management: an overview", Engineering Geology, vol.64, no.1, pp.65-87, 2002.

[13] Asian Development Bank and World Bank (ADB-WB), "Preliminary damage and needs assessment", Asian development bank and world bank, Islamabad, Pakistan, 124, 2005.

[14] W. Chen, W. Li, E. Hou, Z. Zhao, N. Deng, H. Bai, and D. Wang, "Landslide susceptibility mapping based on GIS and information value model for the Chencang District of Baoji, China", Arabian Journal of Geosciences, vol. 7, no. 11, pp. 4499-4511, 2014.

[15] D.P. Kanungo, M.K. Arora, S. Sarkar, and R.P. Gupta, "Landslide susceptibility zonation (LSZ) mapping – a review', Journal of South Asia Disaster Studies, vol. 2, no. 1, pp. 81-105, 2009.

[16] M. Conforti, S. Pascale, G. Robustelli, and F. Sdao, "Evaluation of prediction capability of the artificial neural networks for mapping landslide susceptibility in the Turbolo River catchment (northern Calabria, Italy)", Catena, vol.113, pp. 236-250, 2014.

[17] S. Chakraborty, and R. Pradhan, "Development of GIS-based landslide information system for the region of East Sikkim", International Journal of Computer Applications, vol. 49, no. 7, 2012.

[18] A.N. Khan, A.E. Collins, and F. Qazi," Causes and extent of environmental impacts of landslide hazard in the Himalayan region: a case study of Murree, Pakistan", Natural Hazards, vol. 57, no. 2, pp. 413-434, 2011.

[19] A.N. Khan, and A.U. Rahman "Landslide hazards in the mountainous region of Pakistan", Pakistan Journal of Geography, vol. 16, pp. 38-51, 2006.

[20] J. Choi, H.J. Oh, H.J. Lee, C. Lee, and S. Lee, "Combining landslide susceptibility maps obtained from frequency ratio, logistic regression, and artificial neural network models using ASTER images and GIS", Engineering Geology, vol. 124, pp. 12-23, 2012.

[21] A. Pandey, P.P. Dabral, V.M. Chowdary, and N.K. Yadav, "Landslide hazard zonation using remote sensing and GIS: a case study of Dikrong river basin, Arunachal Pradesh, India", Environmental Geology, vol. 54, no. 7, pp. 1517-1529, 2008.

[22] D. Meghanadh, V.K. Maurya, A. Tiwari, and R. Dwivedi, "A multi-criteria landslide susceptibility mapping using deep multi-layer perceptron network: A case study of Srinagar-Rudraprayag region (India)", Advances in Space Research, vol. 69, no. 4, pp.1883-1893, 2022.

[23] A.S. Dhakal, T. Amada, and M. Aniya, "Landslide hazard mapping and the application of GIS in the Kulekhani watershed, Nepal", Mountain Research and Development, pp. 3-16, 1999.

[24] D.J. Varnes, "Landslide hazard zonation: a review of principles and practice (No. 3)", Natural Hazards, UNESCO, Paris. 1984.

[25] AGS, "Guidelines for landslide susceptibility, hazard and risk zoning for land use planning", Australian Geomechanics. vol. 42, pp. 13–36, 2007.

[26] M.G. Anderson, and E. Holcombe, "Community-based landslide risk reduction-managing disasters in small steps. Library of Congress Cataloging-in-Publication Data", The World Bank, Washington, DC, 2013.

[27] R. Fell, J. Corominas, C. Bonnard, L. Cascini, E. Leroi, and W. Z. Savage, "Guidelines for landslide susceptibility, hazard and risk zoning for land use planning", Engineering Geology, vol. 102, no. 3-4, pp. 85-98, 2008.

[28] M. Shafique, M. van der Meijde, and M.A. Khan, "A review of the 2005 Kashmir earthquake-induced landslides; from a remote sensing perspective", Journal of Asian Earth Sciences, vol. 118, pp. 68-80, 2016.

[29] Y.He, and R.E. Beighley, "GIS-based regional landslide susceptibility mapping: a case study in southern California", Earth Surface Processes and Landforms: The Journal of the British Geomorphological Research Group, vol. 33, no.3, pp. 380-393, 2008.

[30] A. Nandi, and A. Shakoor, "A GIS-based landslide susceptibility evaluation using bivariate and multivariate statistical analyses", Engineering Geology, vol. 110, no. 1-2, pp. 11-20, 2010.

[31] Y. Bahrami, H. Hassani, and A. Maghsoudi, "Landslide susceptibility mapping using AHP and fuzzy methods in the Gilan province, Iran", GeoJournal, vol. 86, pp. 1797–1816, 2020.

[32] P. Kayastha, and M.R. Dhital, F. De-Smedt, "Application of the analytical hierarchy process (AHP) for landslide susceptibility mapping: A case study from the Tinau watershed, west Nepal", Computer Geosciences. Vol. 52, pp. 398–408, 2013.

[33] M. Komac, "A landslide susceptibility model using the analytical hierarchy process method and multivariate statistics in perialpine Slovenia", Geomorphology, vol. 74, no. 1-4, pp. 17-28, 2006.

[34] A. Yalcin, S. Reis, A. C. Aydinoglu, and T. Yomralioglu, "A GIS-based comparative study of frequency ratio, analytical hierarchy process, bivariate statistics and logistics regression methods for landslide susceptibility mapping in Trabzon, NE Turkey". Catena, vol. 85, no. 3, pp. 274-287, 2011.

[35] M.A. Aziz, A.H. Khan, M. Adnan, and H. Ullah, "Traditional uses of medicinal plants used by Indigenous communities for veterinary practices at Bajaur Agency, Pakistan", Journal of ethnobiology and ethnomedicine, vol. 14, no. 1, pp. 1-18, 2018.

[36] A. Mahmood, R.N. Malik, Z.K. Shinwari, and A. Mahmood, "Ethnobotanical survey of plants from Neelum, Azad Jammu and Kashmir, Pakistan", Pakistan Journal of Botany, vol.43, no.10, pp. 10, 2011.

[37] K.S. Ahmad, H. Mansoor, F. Sana, A. Muhammad, A. Farooq, N. Mehwish, Z. Aneela, and A. Iftikhar, "Tribe Andropogoneae from Neelum Valley, Azad Jammu, and Kashmir: Phylogeny Based On Morpho-Anatomy", Pakistan Journal of Botany, vol. 49, pp. 73-82, 2017.

[38] O. Hungr, S. Leroueil, and L. Picarelli, "The Varnes classification of landslide types, an update", Landslides, vol. 11, no. 2, pp. 167-194, 2014.

[39] S. Mandal, and K. Mandal, "Bivariate statistical index for landslide susceptibility mapping in the Rorachu river basin of eastern Sikkim Himalaya, India.", Spatial Information Research, vol. 26.1, pp. 59-75, 2018.

[40] R, Anbalagan, "Landslide hazard evaluation and zonation mapping in mountainous terrain", Engineering Geology, vol. 32, no. 4, pp. 269-277, 1992.

[41] M. Kannan, E. Saranathan, and R. Anabalagan, "Landslide vulnerability mapping using frequency ratio model: a geospatial approach in Bodi-Bodimettu Ghat section, Theni district, Tamil Nadu, India", Arabian Journal of Geosciences, vol. 6, no. 8, pp. 2901-2913, 2013.

[42] M. Ercanoglu, and C. Gokceoglu, "Use of fuzzy relations to produce landslide susceptibility map of a landslide prone area (West Black Sea

Region, Turkey)", Engineering Geology, vol. 75, no. 3-4, pp. 229-250, 2004.

[43] M. Kouli, C. Loupasakis, P. Soupios, and F. Vallianatos, "Landslide hazard zonation in high-risk areas of Rethymno Prefecture, Crete Island, Greece", Natural hazards, vol. 52, no. 3, pp. 599-621, 2010.

[44] Mika, "Weathering of Igneous Rocks" 2013. [Online]. Available: http://wwwgeomikacom/blog/2013/08/17/weathering-igneous/.

[45] A.M. Youssef, M. Al-Kathery, and B. Pradhan, "Landslide susceptibility mapping at Al-Hasher area, Jizan (Saudi Arabia) using GIS-based frequency ratio and index of entropy models", Geosciences Journal, vol. 19, no. 1, pp. 113-134, 2015.

[46] D. Tien Bui, B. Pradhan, I. Revhaug, and C. T. Tran, "A comparative assessment between the application of fuzzy unordered rules induction algorithm and J48 decision tree models in spatial prediction of shallow landslides at Lang Son City, Vietnam", Remote Sensing Applications in Environmental Research, pp. 87-111, 2014.

[47] Q. Wang, W. Li, Y. Wu, Y. Pei, M. Xing, and D. Yang "A comparative study on the landslide susceptibility mapping using evidential belief function and weights of evidence models", Journal of Earth System Science, vol. 125, no. 3, pp. 645-662, 2016.

[48] L. Ayalew, and H. Yamagishi, "The application of GIS-based logistic regression for landslide susceptibility mapping in the Kakuda-Yahiko Mountains, Central Japan", Geomorphology, vol. 65, no. 1-2, pp. 15-31, 2005.

[49] D.T. Bui, B. Pradhan, O. Lofman, I. Revhaug, and O.B. Dick, "Landslide susceptibility assessment in the Hoa Binh province of Vietnam: a comparison of the Levenberg–Marquardt and Bayesian regularized neural networks", Geomorphology, vol. 171, pp. 12-29, 2012.

[50] M. Ercanoglu, and C. Gokceoglu, "Assessment of landslide susceptibility for a landslide-prone area (north of Yenice, NW Turkey) by fuzzy approach", Environmental Geology, vol. 41, no.6, pp. 720-730, 2002.

[51] M.S. Alkhasawneh, U.K. Ngah, L.T. Tay, N.A. M. Isa and M. S. Al-batah, "Determination of important topographic factors for landslide mapping analysis using MLP network", The Scientific World Journal, vol. 2013, pp. 1-12, 2013.

[52] H.J. Oh, and B. Pradhan, "Application of a neuro-fuzzy model to landslide-susceptibility mapping for shallow landslides in a tropical hilly area", Computers & Geosciences, vol. 37, no. 9, pp. 1264-1276, 2011.

[53] S. Singh, "Geomorphology. Allahabad: Prayag Pustak Bhawan," 2000.

[54] S.J. Riley, S.D. DeGloria, and R. Elliot, "Index that quantifies topographic heterogeneity", Intermountain Journal of sciences, vol. 5, no. 1-4, pp. 23-27, 1999.

[55] I.D Moore, and J.P. Wilson, "Length-slope factors for the Revised Universal Soil Loss Equation: Simplified method of estimation", Journal of soil and water conservation, vol. 47, no.5, pp. 423-428, 1992.

[56] H.A. Nefeslioglu, T.Y. Duman, and S. Durmaz, "Landslide susceptibility mapping for a part of tectonic Kelkit Valley (Eastern Black Sea region of Turkey)", Geomorphology, vol. 94, no. 3-4, pp. 401-418, 2008.

[57] S. Himan, K. Saeed, A. Bahrain, and H. Mazlan, "Landslide susceptibility mapping at central Zab basin, Iran: A comparison and ,between analytical hierarchy process, frequency ratio logistic ,70–Catena, vol. 115, pp. 55 ,"regression models2014.

[58] C.W. Chen, H. Saito, and T. Oguchi, "Rainfall intensity–duration conditions for mass movements in Taiwan", Progress in Earth and Planetary Science, vol. 2, no. 1, pp. 1-13, 2015.

[59] P. Biswajeet, and L. Saro, "Utilization of optical remote sensing data and GIS tools for regional landslide hazard analysis by using an artificial neural network model", Earth Sciences. Frontiers. vol. 14, no. 6. pp. 143–152, 2007.

[60] D. Tien Bui, Q.P. Nguyen, N.D. Hoang, and H. Klempe, "A novel fuzzy K-nearest neighbor inference model with differential evolution for spatial prediction of rainfall-induced shallow landslides in a tropical hilly area using GIS", Landslides, vol. 14, no. 1, pp. 1-17, 2017.

[61] L. Lundgren, "Studies of soil and vegetation development on fresh landslide scars in the Mgeta Valley, Western Uluguru Mountains,

Tanzania", Geografiska Annaler: Series A, Physical Geography, vol. 60, no. 3-4, pp. 91-127, 1978.

[62] T. Chen, R. Niu, and X. Jia, "A comparison of information value and logistic regression models in landslide susceptibility mapping by using GIS", Environmental Earth Sciences, vol. 75, no. 10, pp. 867, 2016.

[63] A.M. Eker, M. Dikmen, S. Cambazoğlu, S.H.B. Düzgün, and H. Akgün, "Evaluation and comparison of landslide susceptibility mapping methods: a case study for the Ulus district, Bartın, northern Turkey", International Journal of Geographical Information Science, vol. 29, no. 1, pp. 132-158, 2015.

[64] C. Guo, D.R. Montgomery, Y. Zhang, K. Wang, and Z. Yang, "Quantitative assessment of landslide susceptibility along the Xianshuihe fault zone, Tibetan Plateau, China", Geomorphology, vol. 248, pp. 93-110, 2015.

[65] H. Hong, C. Xu, I. Revhaug, and D. T. Bui, "Spatial prediction of landslide hazard at the Yihuang area (China): a comparative study on the predictive ability of backpropagation multi-layer perceptron neural networks and radial basic function neural networks", In Cartography-maps connecting the world, pp. 175-188, 2015.

[66] S.K. McFeeters, "The use of the Normalized Difference Water Index (NDWI) in the delineation of open water features", International journal of remote sensing, vol. 17, no. 7, pp. 1425-1432, 1996.

[67] A. Yalcin, "GIS-based landslide susceptibility mapping using analytical hierarchy process and bivariate statistics in Ardesen (Turkey): Comparisons of results and confirmations", Catena, vol. 72, pp. 1–12, 2008.

[68] D. Myronidis, C. Papageorgiou, and S. Theophanous, "Landslide susceptibility mapping based on landslide history and analytic hierarchy process (AHP)", Natural Hazards, vol. 81, no. 1, pp. 245–63, 2016.

[69] https://www.arcgis.com/apps/instant/media/index.html

[70] S.M. Fatemi Aghda, V. Bagheri, and M. Razifard, "Landslide susceptibility mapping using the fuzzy logic system and its influences on mainlines in lashgarak region, Tehran, Iran", Geotechnical and Geological Engineering, vol. 36(2), pp. 915-937, 2018.

[71] M. Razifard, G. Shoaei, and M. Zare, "Application of fuzzy logic in the preparation of hazard maps of landslides triggered by the twin Ahar-Varzeghan earthquakes (2012)". Bulletin of Engineering Geology and the Environment, vol. 78(1), pp. 223-245, 2019.

[72] R.H Malik, M. Schouppe, D. Fontan, J. Verkaeren, G. Martinotti, K. H. Shaukat Ahmed, and S. Quresh, "Geology of Neelum valley, district Muzaffarabad, Azad Kashmir, Pakistan", Geological Bulletin, University of Peshawar. vol. 29, pp. 91-111, 1996.

[73] A.M.S Pradhan, and Y.T. Kim, "Relative effect method of landslide susceptibility zonation in weathered granite soil: a case study in Deokjeok-RI Creek, South Korea", Natural hazards, vol. 72, no. 2, pp. 1189-1217, 2014.

[74] V. Ramesh, and S. Anbazhagan, "Landslide susceptibility mapping along Kolli hills Ghat road section (India) using frequency ratio, relative effect, and fuzzy logic models", Environmental Earth Sciences, vol. 73, no. 12, pp. 8009-8021, 2015.

[75] D.W. Hosmer Jr., S. Lemeshow, and R.X. Sturdivant, "Model-building strategies and methods for logistic regression. In: Applied logistic regression, 3rd edn. Wiley, Hoboken, pp 89–151, 2000.

[76] S. Lee, "Application of logistic regression model and its validation for landslide susceptibility mapping using GIS and remote sensing data", International Journal of Remote Sensing, vol.26, no.7, pp. 1477-1491, 2005.